JOURNAL OF EXTRACELLULAR VESICLES
2019, VOL. 8, 1567219
https://doi.org/10.1080/20013078.2019.1567219

Taylor & Francis
Taylor & Francis Group

RESEARCH ARTICLE

OPEN ACCESS Check for updates

An experimental strategy unveiling exosomal microRNAs 486-5p, 181a-5p and 30d-5p from hypoxic tumour cells as circulating indicators of high-risk rectal cancer

Tonje Bjørnetrø [a,b], Kathrine Røe Redalen[a,c], Sebastian Meltzer[a,b], Nirujah Sivarajah Thusyanthan[a], Rampradeep Samiappan[d], Caroline Jegerschöld[d], Karianne Risberg Handeland[a]* and Anne Hansen Ree [a,b]*

[a]Department of Oncology, Akershus University Hospital, Lørenskog, Norway; [b]Institute of Clinical Medicine, University of Oslo, Oslo, Norway; [c]Department of Physics, Norwegian University of Science and Technology, Trondheim, Norway; [d]Department of Bioscience and Nutrition, Karolinska Institutet, Huddinge, Sweden

ABSTRACT

Tumour hypoxia contributes to poor treatment outcome in locally advanced rectal cancer (LARC) and circulating extracellular vesicles (EVs) as potential biomarkers of tumour hypoxia and adverse prognosis have not been fully explored. We examined EV miRNAs from hypoxic colorectal cancer cell lines as template for relevant miRNAs in LARC patients participating in a prospective biomarker study (NCT01816607). Five cell lines were cultured under normoxia (21% O_2) or hypoxia (0.2% O_2) for 24 h, and exosomes were isolated by differential ultracentrifugation. Using a commercial kit, exosomes were precipitated from 24 patient plasma samples collected at the time of diagnosis. Exosome size distribution and protein cargo were determined by cryo-electron microscopy, nanoparticle tracking analysis, immunoblotting and flow cytometry. The vesicles harboured strong cell line-specific miRNA profiles with 35 unique miRNAs differentially expressed between hypoxic and normoxic cells. Six of these miRNAs were considered candidate-circulating markers of tumour hypoxia in the patients based on the frequency or magnitude of variance in hypoxic versus normoxic cell line experiments and prevalence in patient plasma. Of these, low plasma levels of exosomal miR-486-5p and miR-181a-5p were associated with organ-invasive primary tumour ($p = 0.029$) and lymph node metastases ($p = 0.024$), respectively, both attributes of adverse LARC prognosis. In line with this, the plasma level of exosomal miR-30d-5p was elevated in patients who experienced metastatic progression ($p = 0.036$). Our strategy confirmed that EVs from colorectal cancer cell lines were exosomes containing the oxygen-sensitive miRNAs 486-5p, 181a-5p and 30d-5p, which were retrieved as circulating markers of high-risk LARC.

ARTICLE HISTORY
Received 19 April 2018
Revised 3 January 2019
Accepted 5 January 2019

KEYWORDS
Colorectal cancer; extracellular vesicles; hypoxia; miRNA; plasma; rectal cancer; exosomes

Introduction

Solid tumours, including colorectal cancer (CRC), may be heterogeneous with predominant hypoxic regions that develop in poorly vascularised areas and generate an abnormal microenvironment [1]. The insufficient oxygenation activates cellular responses that contribute to the selection of a stress-adapted phenotype of aggressive cancer cells [2,3], which is associated with resistance to cytotoxic therapies (radiation and chemotherapy) and impaired patient survival [4,5]. Hypoxic cells secrete large amounts of exosomes and microvesicles, and these extracellular vesicles (EVs) have been shown to mediate a wide range of paracrine and systemic tissue effects, for example, local tumour angiogenesis and invasiveness as well as distant organ metastasis [6–8].

MicroRNAs (miRNAs) are short RNA species that regulate gene expression at the post-transcriptional level [9]. The expression of miRNAs is altered in tumours compared to normal tissue, with both oncogenic and tumour-suppressor roles attributed [9]. Exosomal miRNAs in the circulation appear remarkably stable and have attained interest as non-invasive biomarkers [10], also in the context of tumour hypoxia, which regulates miRNA transcription and maturation [11,12]. Several studies have investigated exosomal miRNAs as CRC biomarkers [13,14].

Rectal cancer may present as heterogeneous tumours with extensive growth within the pelvic cavity, which are attributes that make this tumour entity a valuable model for investigating biological features associated with tumour hypoxia in a clinical context. Following local

CONTACT Tonje Bjørnetrø bjornetro@gmail.com; tonje.bjornetro@ahus.no Department of Oncology, Akershus University Hospital, P.O. Box 1000, Lørenskog 1478, Norway
*Shared last authorship
Supplemental data for this article can be accessed here

treatment, commonly consisting of neoadjuvant chemoradiotherapy before surgical resection of the residual tumour, the histologic tumour response may vary among patients [15]. Moreover, metastatic progression is a dominant cause of treatment failure [16]. Patients with organ-invasive (denoted T4) or very low (likely involving the anal canal muscles) primary tumour and lymph node metastasis (N-positive disease) in the pelvic cavity are at a particularly high risk of poor treatment outcome [17,18], even though the disease biology shows heterogeneity in this group of patients as a whole. Moreover, recent studies have presented discrepant data as to whether hypoxia as such impacts on local (primary tumour) therapy resistance in rectal cancer [19,20]. All taken into account, readily accessible markers of the hypoxic stress response may provide information about the role of tumour hypoxia and, if decisive for disease outcome, might also assist in stratification of patients with such tumour features into more intensified therapy.

Within this frame of reference, we hypothesised that circulating exosomal miRNA may reflect hypoxic tumour components and as a consequence, imply adverse response to the neoadjuvant treatment and metastatic progression in patients with locally advanced rectal cancer (LARC). Prior to analysis of patient samples, we had to confirm in a pertinent experimental setting that we were handling tumour exosomes as the source of circulating miRNA. Hence, we characterised exosomes and miRNA constituents from five CRC cell lines and found that specific miRNAs were regulated by hypoxia in a cell line-dependent manner. Considered as candidate circulating markers of tumour hypoxia, these exosomal miRNAs were next systematically examined in plasma samples collected from 24 LARC patients at the time of diagnosis and analysed with regard to patient and disease characteristics and treatment outcome. This strategy revealed that exosomal miR-486-5p, miR-181a-5p and miR-30d-5p reflected tumour cell hypoxia and might act as circulating markers of high-risk LARC.

Materials and methods

Cell lines and culture conditions

The human CRC cell lines (HCT116, HCC2998, KM20L2, RKO and LoVo; kindly provided by Prof. Kjersti Flatmark, Oslo University Hospital, Oslo, Norway) were kept in RPMI-1640 medium (Sigma-Aldrich, St. Louis, MO, USA) supplemented with 10% foetal bovine serum (Gibco by Life Technologies, Grand Island, NY, USA) and 2 mM L-glutamine (GE Healthcare–PAA Laboratories, Pashing, Austria) at 37°C in a 5% CO_2 humidified environment. Cell lines were routinely tested and found free of mycoplasma infection, and identity was validated by short tandem repeat analysis. Depending on the cell line, 6–10 × 10^6 cells were seeded in Nunclon T175 flasks (Thermo Fisher Scientific, Waltham, MA, USA). At 70% confluence, cultures were washed three times with PBS (Gibco by Life Technologies) and medium was changed to RPMI-1640 supplemented with 1% bovine serum albumin (BSA; Sigma-Aldrich). In the experimental set-ups, the cells were incubated for 24 h under normoxic (21% O_2) or hypoxic (0.2% O_2) conditions, the latter obtained using the hypoxic chamber Invivo$_2$ 300 (Ruskinn Technologies, Leeds, UK). Cells were harvested using cell scrape, washed in PBS and stored at – 80°C.

Patient material

Citrate plasma samples were collected at study enrolment (the time of diagnosis) from 24 LARC patients participating in a prospective biomarker study (NCT01816607) and prepared according to standardised protocols with centrifugation at 2000× *g* for 10 min followed by storage at – 80°C. The patient population was enrolled from October the 28th, 2013 through August the 18th, 2015. The patients' LARC status was determined by a dedicated multidisciplinary team, which primarily based the decision on disease features revealed by the pelvic magnetic resonance imaging, applying the 2013 ESMO Guidelines [17] (prevailing in the study period) and certain imaging findings that were specified in the updated 2017 version [18]. Hence, the study population came to consist of T2-4N0-2 cases that were considered high-risk: the T2 cases presented a primary tumour threatening the anal levator muscles; the T3 cases had mesorectal fascia margin of 2 mm or less; the T4 cases were defined according to published consensus statements [21]. Survival with or without a metastatic event was censored on February the 14th, 2018, at which time the median follow-up was 33 (range, 9–51) months. The study was approved by the Institutional Review Board and Regional Committee for Medical and Health Research Ethics of South-East Norway (reference number REK 2013/152) and was in accordance with the Declaration of Helsinki. Written informed consent was required for participation.

Exosome preparation

The procedure was modified and based on Crescitelli et al. [22]. Briefly, the conditioned medium was centrifuged at 300× *g* for 10 min to remove floating cells and debris. The supernatant was further centrifuged at 16500× *g* (9600 rpm, *k*-factor 2208) for 20 min using

an AH-629 rotor (Thermo Fisher Scientific) to exclude larger membranous vesicles. To further remove particles, the supernatant was filtered through 0.2-µm Acrodisc filters (Pall Corporation, Ann Arbor, MI, USA) on ice with gentle pressure, and exosomes were pelleted by ultracentrifugation at 151,000× *g* (29000 rpm, *k*-factor 240) for 4 h. The pellet was resolved in PBS or lysed directly, and stored at – 80°C. All centrifugation steps were performed at 4°C. For plasma samples, exosomes were isolated using the miRCURY™ Exosome Isolation Kit (Exiqon Services, Vedbaek, Denmark). In brief, samples were centrifuged at 3000× *g* for 10 min to remove debris and further pre-treated with Thrombin (final concentration of 6 U/mL) before centrifugation at 10000× *g* for 5 min. The samples' supernatants were mixed with precipitation buffer, incubated for 60 min at 4°C and centrifuged at 500× *g* for 5 min. Pellets were dissolved in resuspension buffer and stored at – 80°C.

Immunoblot analysis

Cells and exosomes were lysed in M-PER® Mammalian Protein Extraction Reagent supplemented with Halt™ Protease Inhibitor Cocktail and Halt™ Phosphotase Inhibitor Cocktail (all from Thermo Fisher Scientific). Equal amounts of protein were separated by NuPAGE Bis-Tris (Novex by Life Technologies, Carlsbad, CA, USA) and transferred to Immobilon-P membranes (Millipore Corporation, Billerica, MA, USA). Non-reducing conditions were used for the tetraspanins (CD9, CD63 and CD81). Amido Black (Sigma-Aldrich) was used for total protein staining. The primary antibodies were anti-hypoxia -inducible factor type-1α (HIF1α; 54) (BD Bioscience, San Jose, CA, USA), anti-carbonic anhydrase IX (CAIX; kindly provided by Prof. Silvia Pastorekova, Slovak Academy of Science, Bratislava, Slovak Republic), anti-CD9 (Ts9), anti-CD63 (Ts63) and anti-CD81 (1.3.3.22) (all three from Thermo Fisher Scientific), anti-GRP78 (H-129) (Santa Cruz Biotechnology, Santa Cruz, CA, USA), anti-Alix (3A9) (Abcam, Cambridge, UK), anti-Calnexin (C5C9) and anti-GM130 (D6B1) XP (the two last from Cell Signaling Technology, La Jolla, CA, USA). Secondary antibodies were from Dako Denmark AS (Glostrup, Denmark). Peroxidase activity was visualised using SuperSignal West Dura Extended Duration Substrate (Thermo Fisher Scientific) and ImageQuant Las 3000 system (FujiFilm, Tokyo, Japan).

Cryo-electron microscopy (EM) analysis

Exosome pellets were washed in 0.22-µm-filtered TBS (20 mM) and centrifuged at 151,000× *g* (33,400 rpm, *k*-factor 143) for 140 min at 4°C using a TH-660 rotor (Thermo Fisher Scientific). The pellet was suspended in TBS and stored at – 80°C. Cryo-EM was performed at the Department of Bioscience and Nutrition, Karolinska Institutet, as detailed in Supplemental methods. In brief, the exosome samples (3.5 µL) were applied to holey carbon grids (Quantfoil Micro Tools GmbH, Grosslöbichau, Germany) and plunged into liquid ethane cooled to liquid nitrogen temperature. The vitrified samples were imaged using JEOL 2100F transmission electron microscope (JEOL Ltd., Tokyo) with a 4K × 4K CCD camera (Tietz Video and Imaging Systems GmbH, Germany) at different magnifications.

Nanosight tracking analysis (NTA)

Cell line-derived exosomes were washed in 0.22-µm-filtered PBS and stored at 4°C until analysis. The exosomes were diluted to be within the recommended concentration range and the sample was automatically loaded onto the NS500 instrument (Malvern, Amesbury, UK). Five 60-s videos were captured for each sample during flow mode (camera settings: slide shutter 890, slider gain 146). Plasma-derived exosomes were diluted and loaded onto the NS500 instrument by a syringe at a constant flow of 20. Three 60-s videos were captured for each sample (camera settings: slide shutter 1200, slider gain 146). The videos were analysed with the NTA v3.1 software (Malvern).

Flow-cytometry analysis

Exosome-Human CD81 Flow detection beads (20 µL; Thermo Fisher Scientific) were incubated with 25 µg exosomes for 18–20 h at 4°C. The samples were further incubated for 45–60 min with Phycoerythrin (PE)-labelled mouse anti-human antibodies CD9-PE (M-L13), CD63-PE (H5C6), CD81-PE (JS-81) or an isotype control Mouse IgG1-κ (MOPC-21) (BD Bioscience). The labelled exosomes were analysed with a FACS Diva flow cytometer (BD Bioscience). Data processing was performed with the FlowJo v10 software (Three Star, Inc., Ashland, OR, USA).

miRNA array experiments

The experiments were conducted at Exiqon Services. Total RNA was extracted from cell line-derived exosomes using miRNeasy (Qiagen, Hilden, Germany), according to the manufacturer's instructions. For the plasma exosomes, the miRCURY™ RNA Isolation Kit Biofluids (Exiqon) was used. For each sample, 50 ng RNA were polyadenylated and reverse-transcribed in 50-µL reactions using the miRCURY LNA™ Universal RT microRNA PCR,

Polyadenylation and cDNA Synthesis Kit (Exiqon). cDNA was diluted 50-fold before 10-µL PCR reactions were run on the miRCURY LNA™ Universal RT microRNA PCR Human panel I (Exiqon), which screens 372 human miRNAs. The cell line-derived exosomal miRNAs were analysed in triplicates from each of three independent experiments (for both normoxia and hypoxia), whereas the patient exosomal miRNAs were assessed once per plasma sample. The amplification was performed in a Lightcycler 480 Real-Time PCR System (Roche, Mannheim Germany) on a 384-well plate. In validation experiments, 20 ng RNA in 20-µL cDNA reactions were performed using miScript II RT Kit (Qiagen) and analysed using an alternative PCR system, the miScript PCR Assay (Qiagen). cDNA was diluted 20-fold and analysed in triplicates in 10-µL PCR reactions with primers for miR-30d-5p (MS00003283), miR-30e-5p (MS00007357), miR-31-5p (MS00003290), miR-181a-5p (MS00006685), miR-194-5p (MS00006727), miR-361-3p (MS00009555) and miR-25-3p (MS00003227; reference gene). The amplification was performed in 96 well plates using 7900 HT Fast Real-Time PCR system (Applied Biosystem Foster City, CA, USA). Supplemental methods detail procedures for miRNA quality control and background correction.

miRNA expression analysis

Data normalisation was performed based on the average of the assays detected in each sample (i.e. global mean Cq – assay Cq = dCq), according to Mestdagh et al. [23]. Difference in expression levels was calculated as dCq(1) – dCq(2) = ddCq, where dCq1 and dCq2 correspond to hypoxia and normoxia, respectively, and converted to fold-change by the formula 2^ddCq. The numbers of detected miRNAs were assessed and unsupervised hierarchical clustering was done using R-studio v0.99.903 for Mac and Pheatmap-package v1.0.8 (https://CRAN.R-project.org/package=pheatmap). In the validation experiments, data normalisation was performed using miR-25-3p as reference (normaliser assay Ct – assay Ct = dCt).

Statistical analysis

This was undertaken using IBM SPSS Statistics for Mac v25. For the cell line-derived exosomes, a two-tailed unpaired Student's *t*-test was performed on miRNA sample values only if detected in all of the three biological sample replicates. Patient data were compared using two-tailed Student's *t*-test and correlation between log-transformed continuous data was performed by Pearson product correlation analysis. The values of $p < 0.05$ were considered statistically significant.

Results

Characterisation of normoxic and hypoxic CRC exosomes

Following incubation under normoxic and hypoxic conditions for 24 h, features of isolated EVs were characterised in detail in the HCT116 cell line (Figure 1). First, the intended responses to hypoxia were confirmed by expression of HIF1α and CAIX in hypoxic cells. As expected, no expression of this hypoxia-induced nuclear factor and its target protein was observed in the normoxic cells or in normoxic or hypoxic vesicles (Figure 1(a)). Next, cryo-EM revealed that the isolated EVs were defined by a lipid bilayer and a size of 30–150 nm (Figure 1(b)), and further measurements by NTA showed a vesicle mode size of 144.0 ± 8.78 nm (mean±SEM; $n = 3$) for normoxic cells and 137.6 ± 7.76 nm (mean ± SEM; $n = 3$) for hypoxic cells (Figure 1(c)). Finally, released vesicles from both normoxic and hypoxic HCT116 cells expressed proteins known to be enriched in exosomes (CD9, CD63, CD81 and Alix) and were absent in contamination markers from the endoplasmic reticulum (Calnexin and GRP78) and the Golgi apparatus (GM130), as measured by immunoblot analysis (Figure 1(a); equal protein loading is confirmed in Figure S1 in Supplementary Material) and flow-cytometry analysis (Figure 1(d); examples of gating are shown in Figure S2 in Supplementary Material). Additionally, exosomes harvested from the four other CRC cell lines (HCC2998, KM20L2, LoVo and RKO) also consisted of a lipid bilayer 50–150 nm in size with expression of CD9, CD63 and CD81 (Figure S3 in Supplementary Material).

Exosomal miRNA in CRC cell lines

Next, miRNA was extracted from normoxic and hypoxic exosomes released by the five cell lines and analysed. Cell-free medium supplemented with BSA, as negative control, contained negligible amounts of miRNA (Table S1 in Supplementary Material). For the analysed exosome samples, the average number of detected miRNAs was 211 of the total number of 372 on the panel. Of these, 119 miRNAs were detected in all samples and used for global mean normalisation (Table S2 in Supplementary Material). In unsupervised hierarchical clustering, exosomes harboured strong cell line-specific profiles (Figure S4 in Supplementary Material). However, among the top

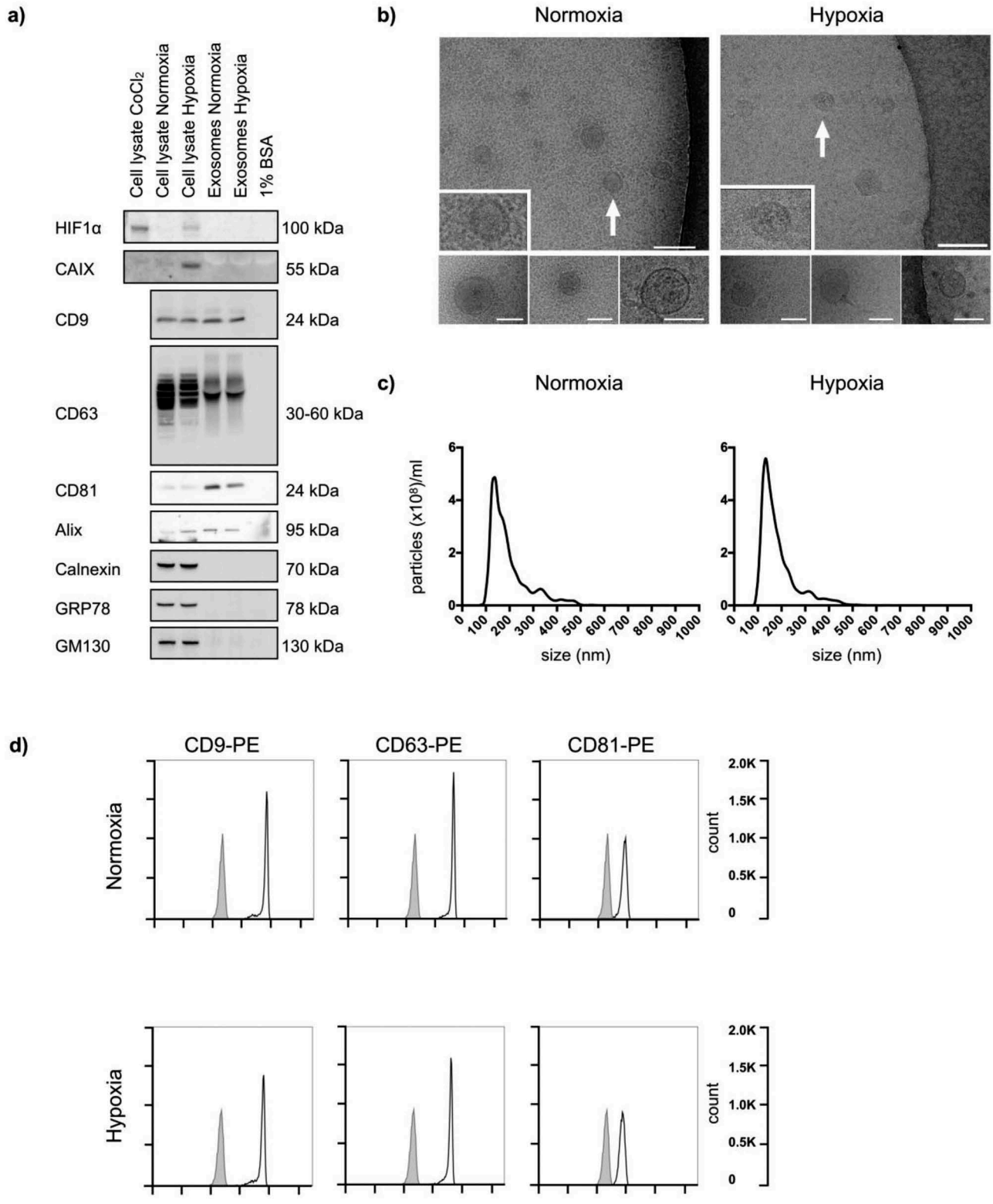

Figure 1. Characteristics of normoxic and hypoxic exosomes released by HCT116 cells. Cells were incubated in medium supplemented with BSA under normoxia or hypoxia for 24 h, and whole cell lysates and extracellular vesicles (EVs) isolated by ultracentrifugation were characterised. For each set of experiments, three biological set-ups were done. (a) Immunoblot images of hypoxia-inducible factor type-1α (HIF1α), carbonic anhydrase IX (CAIX), CD9, CD63, CD81, Alix, Calnexin, GRP78 and GM130 expression. $CoCl_2$ (100 μM for 4 h in normoxia) was positive control for cellular HIF1α expression; culture medium containing 1% BSA was negative control for EVs. 10 μg proteins were loaded in each gel lane. (b) Cryo-electron microscopy images (50,000 ×, 80,000 × and 100,000 × magnifications) of EVs. The positions of the zoomed-in panels within the wide-field views are indicated by arrows; scale bars are 100 nm. The lower panels are independent representative high-magnification images; scale bars are 75 nm. (c) NanoSight tracking histograms of EVs. Mean values from three biological set-ups are shown. (d) Flow-cytometry histograms of EVs stained with Phycoerythrin (PE)-labelled exosome-enriched markers (open traces) or isotype control (filled traces).

10-abundant exosomal miRNAs in each of the five cell lines, and regardless of the oxygenation status, five miRNAs were shared: miR-16-5p, miR-19b-3p, miR-20a-5p, miR-21-5p and miR-106a-5p (Table S3 in Supplementary Material).

As seen from Table 1, a total of 36 unique miRNAs were differently expressed when comparing normoxic and hypoxic exosomes within each of the five cell lines, but only five miRNAs were shared among any two cell lines (miR-29a-3p, miR-181a-5p, miR-194-5p, miR-361-3p and miR-375). Overall, pertaining to single cell lines, 10 miRNAs showed more than 2-fold difference in expression between hypoxic and normoxic exosomes (miR-30d-5p, miR-30e-5p, miR-31-5p, miR-194-5p, miR-361-3p, miR-200c-3p, miR-486-5p, miR-499a-5p, miR-625-3p and miR-663a).

In order to validate differential exosomal expression by an alternative method (the miScript PCR system), six of the miRNAs identified with the miRCURY PCR method (Table 1) were chosen. These were miR-30d-5p, miR-30e-5p, miR-31-5p and miR-181a-5p (down-regulated by hypoxia in the KM20L2 cells) and miR-194-5p and miR-361-3p (up-regulated by hypoxia in the RKO and HCC2998 cell lines, respectively). Altered expression was confirmed for miR-30d-5p (p = 0.028), miR-30e-5p (p = 0.023), miR-31-5p (p = 0.020) and miR-194-5p (p = 0.024), whereas non-significant trends towards hypoxic regulation of exosomal miR-181a-5p (p = 0.27) and miR-361-3p (p = 0.48) were observed (Figure S5 in Supplementary Material).

Table 1. Exosomal microRNAs with significantly different expression by cell lines under hypoxia compared to normoxia.

		FC[a]	p[b]
HCC2998	miR-29a-3p	1.38	0.019
	miR-181a-5p	−1.60	0.0048
	miR-200a-3p	1.26	0.0061
	miR-210-3p	1.65	0.026
	miR-361-3p	1.38	0.032
	miR-365a-3p	1.26	0.0045
	miR-454-3p	1.38	0.027
	miR-499a-5p	3.46	0.023
	miR-671-5p	1.75	0.033
	miR-877-5p	1.21	0.024
HCT116	miR-324-5p	1.56	0.0065
	miR-375	−1.51	0.045
	miR-423-3p	−1.51	0.033
KM20L2	miR-21-5p	−1.09	0.032
	miR-29a-3p	1.39	0.037
	miR-30d-5p	−2.31	0.0077
	miR-30e-5p	−2.16	0.013
	miR-30e-3p	1.26	0.035
	miR-31-5p	−2.07	<0.00001
	miR-99b-5p	−1.51	0.022
	miR-125a-5p	−1.47	0.035
	miR-148b-3p	1.16	0.0069
	miR-181a-5p	−1.15	0.037
	miR-193b-3p	−1.13	0.037
	miR-194-5p	−1.57	0.027
	miR-345-5p	−1.26	0.045
	miR-375	−1.33	0.049
	miR-378a-3p	−1.38	0.0071
	miR-483-3p	1.47	0.048
	miR-598-3p	1.33	0.035
	miR-625-3p	−2.21	0.037
	miR-873-5p	1.50	0.0046
LoVo	miR-22-3p	1.45	0.032
	miR-361-3p	2.95	0.021
	miR-486-5p	−2.18	0.023
	miR-505-3p	−1.50	0.032
	miR-663a	−2.58	0.010
RKO	let-7b-5p	1.38	0.013
	miR-194-5p	2.48	0.033
	miR-200c-3p	2.25	0.042
	miR-221-3p	−1.35	0.033

[a]Fold-change expression in hypoxic versus normoxic exosomes.
[b]By two-tailed unpaired Student's t-test.

Circulating exosomal miRNA in LARC patients

We further investigated whether exosomal miRNAs regulated by hypoxia in CRC cell lines could be retrieved in the circulation of 24 LARC patients at the time of diagnosis, under the following criteria: an equally regulated miRNA shared among any two cell lines detected in at least 75% of patient samples or a miRNA with more than 2-fold change detected in all of the 24 patient samples. In this LARC cohort, 17 (71%) were males and median age was 63 (range, 41–76) years. A considerable number of patients were at particularly high risk, as 14 (58%) had T4 disease and 15 (63%) had local lymph node metastases. Hence, all patients but one received neoadjuvant chemoradiotherapy before surgical resection of the residual tumour; the single case who did not, had the full preoperative radiotherapy but without concomitant radiosensitising chemotherapy because of medical co-morbidity.

EVs were isolated from patients' plasma and samples from three of the patients were used to confirm exosomes. Though the EV quantity and technical quality were suboptimal for the display of EVs isolated from biofluid specimens, cryo-EM analysis revealed that the vesicles consisted of a lipid bilayer 40–70 nm in size (Figure 2(a)). The NTA showed a diameter of 111.3 ± 7.76 nm (mean ± SEM; n = 3) (Figure 2(b)). The vesicles were positive for CD9, CD63 and Alix expression and negative for GM130 by immunoblot analysis (Figure 2(c)). The average number of detected exosomal miRNAs in the patient samples was 138 (of 372 on the panel), of which 48 were shared among all patients and used for global mean normalisation (Table S2 in Supplementary Material). Furthermore, among the top 10-abundant miRNAs, six were also found on the list of top 10-abundant exosomal miRNAs from the cell lines (miR-16-5p, miR-19b-3p, miR-20a-5p, miR-21-5p, miR-23a-3p and miR-24-3p; Table S3 in Supplementary Material).

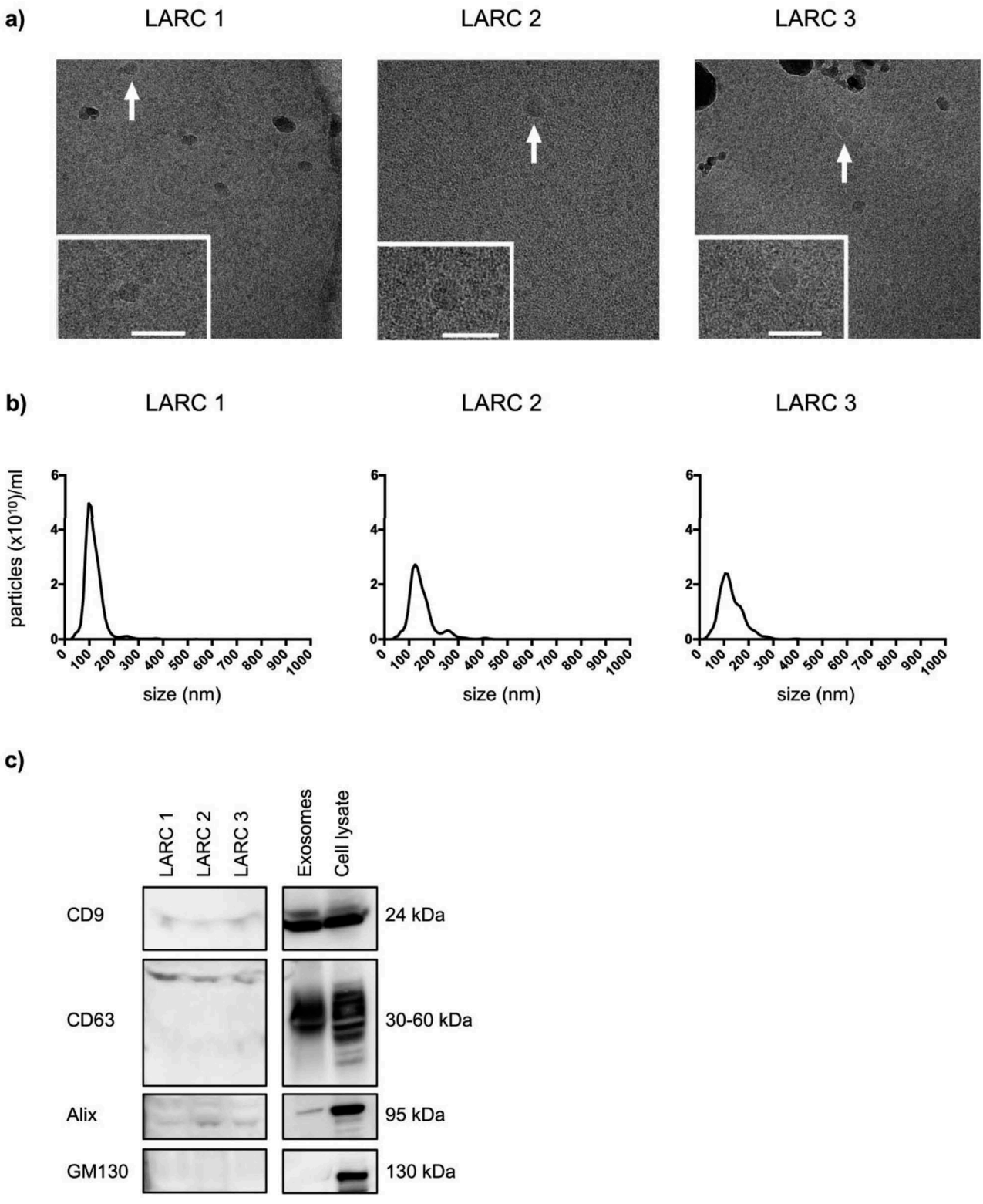

Figure 2. Characteristics of circulating exosomes from patients with locally advanced rectal cancer (LARC). Extracellular vesicles (EVs) precipitated from three patients' plasma samples by the miRCURY™ Exosome Isolation Kit (Exiqon Services) were characterised. (a) Cryo-electron microscopy images (50,000 × and 60,000 × magnifications) of EVs. The dark grey structures are ice crystal contaminations (in LARC 1 and LARC 3). The positions of the zoomed-in panels within the wide-field views are indicated by arrows; scale bars are 100 nm. (b) NanoSight tracking histogram of EVs. (c) Immunoblot images of CD9, CD63, Alix and GM130 expression. Whole cell lysates and exosomes isolated by ultracentrifugation from the HCT116 cell line were controls. 150 µg proteins from the EV plasma samples and 10 µg proteins from the cell line samples were loaded on the gel.

When applying the selection criteria, three of the five shared oxygen-sensitive exosomal miRNAs from cell lines were detected in the sufficient number of patient samples (miR-29a-3p, miR-181a-5p and miR-375) and also three of the 10 miRNAs with more than 2-fold alteration were detected in circulation of all patients (miR-30d-5p, miR-30e-5p and miR-486-5p); Figure S6 in Supplementary Material provides a graphical representation of all the data. Exosomal miR-194-5p was ignored for analysis in patient samples as it was both up-regulated and down-regulated in response to hypoxia in cell lines. As presented in Table 2, circulating levels of miR-486-5p (repressed in hypoxic cell line exosomes; Table 1) were lower in patients with organ-invasive primary tumour (T4) than in T2-3 cases ($p = 0.029$). Likewise, exosomal miR-181a-5p levels (repressed in hypoxic cell line exosomes; Table 1) were lower in patients with pelvic lymph node metastases than in those without ($p = 0.024$). Intriguingly, exosomal miR-30d-5p levels (repressed in hypoxic cell line exosomes; Table 1) were higher in patients who developed metastatic disease ($p = 0.036$); seven of the nine cases had liver metastases. Circulating levels of the remaining three miRNAs that met the selection criteria for investigation did not show any association with TN status or metastatic progression (Table 2). Importantly, there was no correlation between any of the six selected miRNAs and local tumour response to the neoadjuvant treatment (denoted as ypTN stage; regarded a surrogate marker for long-term outcome [24]), as shown in Table 2. As shown in Table S4 in Supplementary Material, circulating levels of the six selected miRNAs were not associated with sex, age or body mass index. However, an inverse correlation ($r = -0.46$, $p = 0.029$) was found between the levels of miR-181a-5p and carcinoembryonic antigen, a CRC marker used in routine practice [25].

Discussion

In this study, we used a commercial platform to analyse miRNA profiles of exosomes released from five hypoxic CRC cell lines as template for circulating exosomal miRNA in LARC patients. A set of exosomal miRNAs was selected based on the frequency or magnitude of variance in hypoxic versus normoxic cell line experiments and prevalence in patient plasma. By this approach, we identified six candidate oxygen-sensitive exosomal miRNAs from the cell lines, which could be analysed with regard to patients' TN status at diagnosis and outcome. Of these, low levels of miR-486-5p and miR-181a-5p were associated with T4 and N-positive disease, respectively, and high exosomal miR-30d-5p level with metastatic progression. Our strategy revealed circulating exosomal indicators of tumour hypoxia that might inform on LARC outcome.

The approach relied on the verification that the circulating EVs represented exosomes. First, during the experimental set-ups, the CRC cell lines were kept in medium without serum to avoid bovine exosome contamination [26]. The five cell lines were chosen

Table 2. Exosomal microRNAs in patients' plasma and correlations with disease factors.

		n	Mean (SD)	p^a	*n*	Mean (SD)	p^a	*n*	Mean (SD)	p^a
			miR-29a-3p			miR-181a-5p			miR-375	
T stage	2–3	6	−0.981 (0.538)		9	−2.14 (0.359)		8	−3.28 (1.51)	
	4	12	−1.05 (0.480)	0.79	14	−2.12 (1.09)	0.95	12	−3.39 (1.11)	0.85
N stage	0	5	−1.18 (0.643)		9	−1.64 (0.757)		7	−3.35 (0.928)	
	1–2	13	−0.969 (0.427)	0.44	14	−2.45 (0.796)	0.024	13	−3.34 (1.43)	0.98
ypT stage	0–2	5	−0.943 (0.577)		7	−1.70 (0.653)		8	−3.29 (1.25)	
	3–4	13	−1.06 (0.467)	0.66	16	−2.32 (0.893)	0.11	12	−3.38 (1.30)	0.87
ypN stage	0	8	−0.996 (0.425)		11	−2.13 (1.10)		9	−3.34 (0.535)	
	1–2	10	−1.05 (0.550)	0.82	12	−2.13 (0.623)	0.99	11	−3.34 (1.65)	1.0
Metastasis	No	11	−0.974 (0.506)		14	−1.98 (0.876)		12	−3.57 (1.25)	
	Yes	7	−1.11 (0.475)	0.58	9	−2.37 (0.839)	0.31	8	−3.00 (1.24)	0.32
			miR-30d-5p			miR-30e-5p			miR-486-5p	
T stage	2-3	10	−1.20 (1.24)		10	−0.469 (0.515)		10	1.37 (0.360)	
	4	14	−0.546 (0.666)	0.11	14	−0.420 (0.380)	0.79	14	1.03 (0.343)	0.029
N stage	0	9	−0.536 (0.759)		9	−0.439 (0.521)		9	1.28 (0.369)	
	1–2	15	−0.988 (1.08)	0.28	15	−0.442 (0.388)	0.99	15	1.10 (0.388)	0.28
ypT stage	0–2	8	−1.11 (1.44)		8	−0.433 (0.529)		8	1.24 (0.326)	
	3–4	16	−0.671 (0.657)	0.43	16	−0.445 (0.393)	0.95	16	1.13 (0.413)	0.51
ypN stage	0	11	−0.691 (0.680)		11	−0.401 (0.496)		11	1.17 (0.301)	
	1–2	13	−0.926 (1.19)	0.57	13	−0.474 (0.386)	0.69	13	1.17 (0.453)	0.99
Metastasis	No	15	−1.09 (1.15)		15	−0.431 (0.387)		15	1.24 (0.375)	
	Yes	9	−0.373 (0.300)	0.036	9	−0.456 (0.510)	0.89	9	1.05 (0.387)	0.26

[a]By two-tailed Student's *t*-test.
SD, standard deviation; TN, tumour-node; yp, histologic response to neoadjuvant therapy.

based on their tolerance to 24 h of hypoxia in BSA-containing medium (data not shown). The cell line-derived exosomes were isolated by ultracentrifugation and thoroughly characterised. Still, this isolation method may have resulted in different EV populations from the various cell lines because the sedimentation rate is dependent on shape and mass density [27], and co-precipitation of protein aggregates and other carriers of extracellular miRNA might have contaminated the final samples [28]. We chose to precipitate EVs from the plasma specimens with a commercial kit as it is less time-consuming and technique-sensitive and better adapted to small sample volumes. This easy and fast protocol performed well in a comparative study of ultracentrifugation and commercial reagents [29].

The observed miRNA alterations might result from differences in either exosome or miRNA abundance, or both. Exosomal RNA isolation from the conditioned media and plasma specimens was performed with two different kits. Although we found considerable similarity of the top 10-abundant miRNAs between the experimental and clinical models, we cannot rule out differences in miRNA retrieval by the two methods. Nevertheless, the findings strongly indicate that circulating miRNA detected in LARC patients stemmed from their rectal tumour. In further support of this, several reports have demonstrated many of the same miRNAs at higher occurrence in circulating EVs from CRC patients compared to healthy controls, with significant reduction of the miRNAs after resection of the primary tumour [30–32]. As far as we know, our study is the first to compare exosomal miRNA profiles from hypoxic CRC cell lines with the normoxic counterparts. Not surprisingly, profiles were primarily cell line-specific, commonly seen in intracellular miRNA profiles of hypoxic CRC cell lines [33]. Among the oxygen-sensitive exosomal miRNAs we identified, several have been reported as hypoxia-regulated in processes such as autophagy [34,35], angiogenesis [36,37], extracellular matrix synthesis [38] and liver fibrosis [39]. Overall, the majority of the detected exosomal miRNAs were not altered by hypoxia. We did not analyse the cell line miRNA signatures upon a return from hypoxia to normoxia. From a technical point of view, we aimed to validate six oxygen-sensitive miRNAs with a different PCR platform, for four of which the exosomal expression was confirmed statistically different. Of additional technical note, the studied miRNAs might have been attached to the outside of or otherwise co-isolated with the exosomes [40], although this to have occurred with both of the EV isolation protocols seems unlikely.

Moreover, biological functions of miRNAs are commonly dependent on the local cellular context, which conceptually poses challenges to using cell lines as models of biomarkers relevant for a clinical circumstance. It is unclear to which extent primary LARC tumours with anatomically aggressive features (T4 or N-positive disease) are hypoxic, and further how tumour hypoxia impacts on the local therapy response [19,20]. Our investigations did not show any correlation between the exosomal miRNAs selected based on cell line hypoxia and local tumour response to the neoadjuvant treatment (ypTN stage), which if present would have indicated a paracrine tissue effect of the actual miRNAs.

Circulating levels of exosomal miR-486-5p were lower in the group of LARC patients with T4 disease than in T2-3 cases, the former presenting more advanced primary tumour within the pelvic cavity. Others have reported that tissue miR-486-5p expression is gradually declining from normal bowel mucosa via early-stage CRC to advanced disease, and that this miRNA suppresses tumour growth and lymphangiogenesis [41]. A similar tumour-suppressor role of miR-486-5p has also been seen in lung and gastric cancer [42,43]. In apparent contrast to our cell line exosomal data, hypoxia in mesenchymal stem cells caused enhancement of intracellular miR-486, promoting proliferation and angiogenic activity [44]. Moreover, in erythroleukemia cells, hypoxia was shown to increase both intracellular and exosomal miR-486 [45].

Circulating levels of exosomal miR-181a-5p were lower in the group of LARC patients with pelvic lymph node metastases than in cases without, the former predicting adverse prognosis. The finding was supported by the inverse correlation between this miRNA and the circulating tumour marker carcinoembryonic antigen. In CRC, miR-181a has been investigated as prognostic biomarker, but with conflicting results; a recent meta-analysis showed that high tumour levels of miR-181a predicted poor overall survival [46]. An interesting study of colon cancer specimens showed elevated expression of a major proteinase involved in extracellular matrix remodelling at the invasive tumour front where miR-181a-5p expression was repressed relative to the adjacent normal tissue [47]. In further support of a tumour-suppressor role, induction of miR-181a-5p in CRC cell lines restrained their proliferation and chemotherapy resistance [48].

While miR-30d-5p was repressed in hypoxic cell line exosomes, its plasma levels were higher in the group of LARC patients who had developed

metastatic disease than in those who had not progressed at the time of censoring, which seemingly were contradictory findings. Supporting our patient data, a recent report showed that miR-30d expression was high in hypoxic CRC cell lines and in primary tumours from patients who failed adjuvant therapy (presumably by metastatic progression, but not specified [33]). In hepatocellular carcinoma, miR-30d was shown to be highly expressed [49–51] and promote intrahepatic tumour cell invasion and implant tumours [49]. Interestingly, the great majority of the metastatic cases in the present study had dissemination to the liver, suggesting that circulating exosomal miR-30d-5p from their primary tumours may have contributed to this organ-specificity of metastasis [52].

In conclusion, acknowledging that the patient cohort was small and correction for multiple testing was not done, our hypothesis confirmed that CRC cell line EVs including exosomes contained the oxygen-sensitive miRNAs 486-5p, 181a-5p and 30d-5p, which were retrieved as circulating markers of high-risk LARC. This particular strategy may show useful for studying the clinical role of hypoxia-adapted phenotypes in several tumour entities.

Acknowledgements

The authors acknowledge the generous gift of the carbonic anhydrase IX antibody from Prof. Silvia Pastorekova, Slovak Academy of Science and the assistance in the NanoSight tracking analyses by Dr. Alicia Llorente and Mrs. Anne-Marie Siebke Trøseid, Oslo University Hospital.

Disclosure statement

No potential conflict of interest was reported by the authors.

Funding

This work was supported by the South-Eastern Norway Regional Health Authority [grant number 2013002], [grant number 2014010], [grant number 2016050], [grant number 2017109]; Akershus University Hospital [grant number 2017013], [grant number 2018004]; the Karolinska Institute contribution under the Science Council [grant number 2016-03810]; and a Centre for Innovative Medicine Grant.

ORCID

Tonje Bjørnetrø http://orcid.org/0000-0003-2110-5875
Anne Hansen Ree http://orcid.org/0000-0002-8264-3223

References

[1] Axelson H, Fredlund E, Ovenberger M, et al. Hypoxia-induced dedifferentiation of tumor cells–a mechanism behind heterogeneity and aggressiveness of solid tumors. Semin Cell Dev Biol. 2005;16(4–5):554–563.
[2] Harris AL. Hypoxia–a key regulatory factor in tumour growth. Nat Rev Cancer. 2002;2(1):38–47.
[3] Marusyk A, Almendro V, Polyak K. Intra-tumour heterogeneity: a looking glass for cancer? Nat Rev Cancer. 2012;12(5):323–334.
[4] Doktorova H, Hrabeta J, Khalil MA, et al. Hypoxia-induced chemoresistance in cancer cells: the role of not only HIF-1. Biomed Pap Med Fac Univ Palacky Olomouc Czech Repub. 2015;159(2):166–177.
[5] Wigerup C, Pahlman S, Bexell D. Therapeutic targeting of hypoxia and hypoxia-inducible factors in cancer. Pharmacol Ther. 2016;164:152–169.
[6] Belting M, Christianson HC. Role of exosomes and microvesicles in hypoxia-associated tumour development and cardiovascular disease. J Intern Med. 2015;278(3):251–263.
[7] King HW, Michael MZ, Gleadle JM. Hypoxic enhancement of exosome release by breast cancer cells. BMC Cancer. 2012;12:421.
[8] Park JE, Tan HS, Datta A, et al. Hypoxic tumor cell modulates its microenvironment to enhance angiogenic and metastatic potential by secretion of proteins and exosomes. Mol Cell Proteomics. 2010;9(6):1085–1099.
[9] Peng Y, Croce CM. The role of MicroRNAs in human cancer. Signal Transduct Target Ther. 2016;1:15004.
[10] Lan H, Lu H, Wang X, et al. MicroRNAs as potential biomarkers in cancer: opportunities and challenges. Biomed Res Int. 2015;2015:125094.
[11] Nallamshetty S, Chan SY, Loscalzo J. Hypoxia: a master regulator of microRNA biogenesis and activity. Free Radic Biol Med. 2013;64:20–30.
[12] Shen G, Li X, Jia YF, et al. Hypoxia-regulated microRNAs in human cancer. Acta Pharmacol Sin. 2013;34(3):336–341.
[13] Tovar-Camargo OA, Toden S, Goel A. Exosomal microRNA biomarkers: emerging Frontiers in colorectal and other human cancers. Expert Rev Mol Diagn. 2016;16(5):553–567.
[14] Hon KW, Abu N, Ab Mutalib NS, et al. Exosomes as potential biomarkers and targeted therapy in colorectal cancer: a mini-review. Front Pharmacol. 2017;8:583.
[15] Franke AJ, Parekh H, Starr JS, et al. Total neoadjuvant therapy: a shifting paradigm in locally advanced rectal cancer management. Clin Colorectal Cancer. 2018;17(1):1–12.
[16] Bosset JF, Calais G, Mineur L, et al. Fluorouracil-based adjuvant chemotherapy after preoperative chemoradiotherapy in rectal cancer: long-term results of the EORTC 22921 randomised study. Lancet Oncol. 2014;15(2):184–190.
[17] Glimelius B, Tiret E, Cervantes A, et al. Rectal cancer: ESMO clinical practice guidelines for diagnosis, treatment and follow-up. Ann Oncol. 2013;24(Suppl 6):81–88.
[18] Glynne-Jones R, Wyrwicz L, Tiret E, et al. Rectal cancer: ESMO clinical practice guidelines for diagnosis,

treatment and follow-up. Ann Oncol. 2017;28(Suppl 4):22–40.
[19] Lee-Kong SA, Ruby JA, Chessin DB, et al. Hypoxia-related proteins in patients with rectal cancer undergoing neoadjuvant combined modality therapy. Dis Colon Rectum. 2012;55(9):990–995.
[20] Verstraete M, Debucquoy A, Dekervel J, et al. Combining bevacizumab and chemoradiation in rectal cancer. Translational results of the AXEBeam trial. Br J Cancer. 2015;112(8):1314–1325.
[21] Beyond TME Collaborative. Consensus statement on the multidisciplinary management of patients with recurrent and primary rectal cancer beyond total mesorectal excision planes. Br J Surg. 2013;100(8):1009–1014.
[22] Crescitelli R, Lasser C, Szabo TG, et al. Distinct RNA profiles in subpopulations of extracellular vesicles: apoptotic bodies, microvesicles and exosomes. J Extracell Vesicles. 2013;2:1.
[23] Mestdagh P, van Vlierberghe P, de Weer A, et al. A novel and universal method for microRNA RT-qPCR data normalization. Genome Biol. 2009;10(6):R64.
[24] Aklilu M, Eng C. The current landscape of locally advanced rectal cancer. Nat Rev Clin Oncol. 2011;8(11):649–659.
[25] Lech G, Slotwinski R, Slodkowski M, et al. Colorectal cancer tumour markers and biomarkers: recent therapeutic advances. World J Gastroenterol. 2016;22(5):1745–1755.
[26] Wei Z, Batagov AO, Carter DR, et al. Fetal bovine serum RNA interferes with the cell culture derived extracellular RNA. Sci Rep. 2016;6:31175.
[27] Jeppesen DK, Hvam ML, Primdahl-Bengtson B, et al. Comparative analysis of discrete exosome fractions obtained by differential centrifugation. J Extracell Vesicles. 2014;3:25011.
[28] Witwer KW, Buzas EI, Bemis LT, et al. Standardization of sample collection, isolation and analysis methods in extracellular vesicle research. J Extracell Vesicles. 2013;2(1).
[29] Helwa I, Cai J, Drewry MD, et al. A comparative study of serum exosome isolation using differential ultracentrifugation and three commercial reagents. PLoS One. 2017;12(1):e0170628.
[30] Ostenfeld MS, Jensen SG, Jeppesen DK, et al. miRNA profiling of circulating EpCAM(+) extracellular vesicles: promising biomarkers of colorectal cancer. J Extracell Vesicles. 2016;5:31488.
[31] Zhu M, Huang Z, Zhu D, et al. A panel of microRNA signature in serum for colorectal cancer diagnosis. Oncotarget. 2017;8(10):17081–17091.
[32] Ogata-Kawata H, Izumiya M, Kurioka D, et al. Circulating exosomal microRNAs as biomarkers of colon cancer. PLoS One. 2014;9(4):e92921.
[33] Nijhuis A, Thompson H, Adam J, et al. Remodelling of microRNAs in colorectal cancer by hypoxia alters metabolism profiles and 5-fluorouracil resistance. Hum Mol Genet. 2017;26(8):1552–1564.
[34] Chang Y, Yan W, He X, et al. miR-375 inhibits autophagy and reduces viability of hepatocellular carcinoma cells under hypoxic conditions. Gastroenterology. 2012;143(1):177–87 e8.
[35] Chakrabarti M, Klionsky DJ, Ray SK. miR-30e blocks autophagy and acts synergistically with proanthocyanidin for inhibition of AVEN and BIRC6 to increase apoptosis in glioblastoma stem cells and glioblastoma SNB19 cells. PLoS One. 2016;11(7):e0158537.
[36] Yang Z, Wu L, Zhu X, et al. MiR-29a modulates the angiogenic properties of human endothelial cells. Biochem Biophys Res Commun. 2013;434(1):143–149.
[37] Dal Monte M, Landi D, Martini D, et al. Antiangiogenic role of miR-361 in human umbilical vein endothelial cells: functional interaction with the peptide somatostatin. Naunyn Schmiedebergs Arch Pharmacol. 2013;386(1):15–27.
[38] Wang X, Zhang Y, Jiang BH, et al. Study on the role of Hsa-miR-31-5p in hypertrophic scar formation and the mechanism. Exp Cell Res. 2017;361(2):201–209.
[39] Hu J, Chen C, Liu Q, et al. The role of the miR-31/FIH1 pathway in TGF-beta-induced liver fibrosis. Clin Sci (Lond). 2015;129(4):305–317.
[40] Hill AF, Pegtel DM, Lambertz U, et al. ISEV position paper: extracellular vesicle RNA analysis and bioinformatics. J Extracell Vesicles. 2013;2(1):22859.
[41] Liu C, Li M, Hu Y, et al. miR-486-5p attenuates tumor growth and lymphangiogenesis by targeting neuropilin-2 in colorectal carcinoma. Onco Targets Ther. 2016;9:2865–2871.
[42] Wang J, Tian X, Han R, et al. Downregulation of miR-486-5p contributes to tumor progression and metastasis by targeting protumorigenic ARHGAP5 in lung cancer. Oncogene. 2014;33(9):1181–1189.
[43] Oh HK, Tan AL, Das K, et al. Genomic loss of miR-486 regulates tumor progression and the OLFM4 antiapoptotic factor in gastric cancer. Clin Cancer Res. 2011;17(9):2657–2667.
[44] Shi XF, Wang H, Xiao FJ, et al. MiRNA-486 regulates angiogenic activity and survival of mesenchymal stem cells under hypoxia through modulating Akt signal. Biochem Biophys Res Commun. 2016;470(3):670–677.
[45] Shi XF, Wang H, Kong FX, et al. Exosomal miR-486 regulates hypoxia-induced erythroid differentiation of erythroleukemia cells through targeting Sirt1. Exp Cell Res. 2017;351(1):74–81.
[46] Gu X, Jin R, Mao X, et al. Prognostic value of miRNA-181a/b in colorectal cancer: a meta-analysis. Biomark Med. 2018;12(3):299–308.
[47] Li Y, Kuscu C, Banach A, et al. miR-181a-5p inhibits cancer cell migration and angiogenesis via downregulation of matrix metalloproteinase-14. Cancer Res. 2015;75(13):2674–2685.
[48] Han P, Li JW, Zhang BM, et al. The lncRNA CRNDE promotes colorectal cancer cell proliferation and chemoresistance via miR-181a-5p-mediated regulation of Wnt/beta-catenin signaling. Mol Cancer. 2017;16(1):9.
[49] Yao J, Liang L, Huang S, et al. MicroRNA-30d promotes tumor invasion and metastasis by targeting Galphai2 in hepatocellular carcinoma. Hepatology. 2010;51(3):846–856.

[50] Liu AM, Zhang C, Burchard J, et al. Global regulation on microRNA in hepatitis B virus-associated hepatocellular carcinoma. OMICS. 2011;15(3):187–191.
[51] Cervantes-Anaya N, Ponciano-Gomez A, Lopez-Alvarez GS, et al. Downregulation of sorting nexin 10 is associated with overexpression of miR-30d during liver cancer progression in rats. Tumour Biol. 2017;39(4):1010428317695932.
[52] Peinado H, Zhang H, Matei IR, et al. Pre-metastatic niches: organ-specific homes for metastases. Nat Rev Cancer. 2017;17(5):302–317.